galaxies

MDPI

Article

Direct Imaging of the Cosmic Battery in M87*? Not Yet

Ioannis Contopoulos [1,*,†], Ioannis Myserlis [2,†], Demosthenes Kazanas [3,†] and Antonios Nathanail [4,†]

1 Research Center for Astronomy and Applied Mathematics, Academy of Athens, 11527 Athens, Greece
2 Institut de Radioastronomie Millimétrique, Avenida Divina Pastora 7, Local 20, 18012 Granada, Spain; imyserlis@iram.es
3 Astrophysics Science Division, NASA/Goddard Space Flight Center, Greenbelt, MD 20771, USA; demos.kazanas@nasa.gov
4 Department of Physics, National and Kapodistrian University of Athens, Panepistimiopolis, 15783 Zografos, Greece; antonionitoni@hotmail.com
* Correspondence: icontop@academyofathens.gr
† These authors contributed equally to this work.

Abstract: One of the fundamental conclusions of the Cosmic Battery (a means for producing poloidal magnetic flux in the vicinity of a black hole via the Poynting-Robertson effect on the accretion disk) is that it determines the direction of the axial magnetic field: near the black hole it is parallel to the angular velocity Ω of the surrounding disk, while further away it is anti-parallel to Ω. The EHT polarization observations of M87* where the innermost accretion disk is observed almost face-on thus offer an ideal opportunity to study the action of the Cosmic Battery, by deciding whether the field geometry is consistent with its premises. Unfortunately, such a determination is difficult at the moment due to the lack of reliable Faraday Rotation Measure (RM) maps of M87* at event horizon scales. Furthermore, in agreement with recent General Relativistic Magnetohydrodynamic (GRMHD) numerical simulations, if the inner accretion disk is highly turbulent, one would expect the RM to flip sign on dynamical time scales. While such RM observations are paramount for the determination of the field geometry in confirmation or refutation of the Cosmic Battery, this may have to wait for long term monitoring at event horizon scales and perhaps the synergy of lower resolution RM observations.

Keywords: EHT–M87*–magnetic fields–stars; black holes

check for updates

Citation: Contopoulos, I.; Myserlis, I.; Kazanas, D.; Nathanail, A. Direct Imaging of the Cosmic Battery in M87*? Not Yet. *Galaxies* **2022**, *10*, 80. https://doi.org/10.3390/galaxies10040080

Academic Editors: Jaziel Goulart Coelho and Rita C. Anjos

Received: 30 May 2022
Accepted: 23 June 2022
Published: 29 June 2022

1. Introduction

The Event Horizon Telescope (EHT) Collaboration has recently published polarization images of the event-horizon-scale emission around the supermassive black hole at the center of the M87 galaxy (M87*; [1,2]). The images reveal that a significant fraction of the emission is linearly polarized, as expected for synchrotron emission from relativistic electrons gyrating around well organized magnetic field lines in the M87 jet and/or the surrounding accretion disk. The sign of the Faraday Rotation Measure (RM) derived from these images determines the direction of the magnetic field that threads the disk: by convention, negative values correspond to an average magnetic field pointing *away from* the observer, while positive values *towards* the observer. The M87 jet points towards us at 17° to our line-of-sight, and the disk around M87* rotates in the clockwise direction in the plane of the sky [3]. This offers a unique opportunity to test the Cosmic Battery model for the origin of magnetic fields around astrophysical black holes which surmises that the large scale axial magnetic field in the immediate vicinity of the M87* black hole points away from us (along the direction of Ω of the disk), while further away it points towards us[1].

In the next Section, we will present a rough prediction for the distribution of the axial magnetic field around the central black hole according to the Cosmic Battery. We will then provide the general features of an RM map of the average axial field whenever it will become reliably available. In Section 3 we discuss that, in order to confirm the prediction of the Cosmic Battery, we are only interested to know whether the average

line-of-sight magnetic field changes direction at some particular distance from the center. Episodic enhancement of the radiation in such regions of opposite line-of-sight magnetic field direction could give rise to the observed rapid flips in the sign of the average RM [5]. However, these RM sign flips may also have to do with the turbulent events observed in the General Relativistic Magnetohydrodynamic (GRMHD) numerical simulations of [6]. Further monitoring of the polarization emission of M87* as well as polarization angle observations over a wider frequency range will help disentangle between these possible scenarios. We conclude in Section 4 with a discussion of the prospects for testing the Cosmic Battery.

2. RM Map According to the Cosmic Battery

The Cosmic Battery model for the generation of poloidal magnetic fields around astrophysical black holes was first proposed by Contopoulos & Kazanas [7]. According to that mechanism, the aberrated radiation pressure on the electrons of the electron-proton plasma in orbit around the black hole decelerates the electrons and thus induces an azimuthal electric field opposite to the direction of rotation. The rotation (curl) of this electric field generates poloidal magnetic field flux which, near the black hole, is along the direction of disk-hole rotation Ω ('magnetism along spin', [8]), and in the surrounding disk is opposite to Ω (e.g., [9,10]). In a disk that is observed almost face-on with Ω pointing away from us (as is the case with the clockwise rotating disk of M87*), one expects that the central parts of the image will show generally negative RM values, whereas the outer parts of the image will consistently show generally positive RM values.

In order to generate theoretical RM maps, we will use a simple model for the distribution of electron density $n_{\rm e}$ and axial magnetic field B_z with distance R in the equatorial plasma disk of M87*. We will thus assume that $n_{\rm e}$ drops exponentially inside the distance of field reversal $R_{\rm CB}$, and inversely with distance outside. Similarly, we will assume that B_z stays roughly constant inside $R_{\rm CB}$, and also drops inversely with distance outside, according to the observational conclusions of Fukumura et al. [11] on self-similar magnetic winds from astrophysical accretion disks. The distance $R_{\rm CB}$ is currently a big unknown that will be determined with more numerical simulations analogous to those of [12]. Finally, we will assume that most of the contribution to the RM comes from a thin disk with scale-height/thickness that increases proportionally with distance R from the center. We will thus consider the ad hoc expressions

$$n_{\rm e}(R) = \begin{cases} n_{{\rm e}o}\,{\rm e}^{-\frac{|R-R_{\rm CB}|}{2}} & \text{inside } R_{\rm CB} \\ n_{{\rm e}o}\,\frac{R_{\rm CB}}{R} & \text{outside } R_{\rm CB} \end{cases} \tag{1}$$

$$B_z(R) = \begin{cases} -B_{zo} & \text{inside } R_{\rm CB} \\ B_{zo}\,\frac{R_{\rm CB}}{R} & \text{outside } R_{\rm CB} \end{cases} \tag{2}$$

$$h(R) = h_o\,\frac{R}{R_{\rm CB}} \tag{3}$$

If we were to observe such a magnetic field/plasma distribution face-on from below, this would yield

$${\rm RM}_{\rm face-on}(R) = \begin{cases} -{\rm RM}_o\,\frac{R}{R_{\rm CB}}\,{\rm e}^{-\frac{|R-R_{\rm CB}|}{2}} & \text{inside } R_{\rm CB} \\ {\rm RM}_o\,\frac{R_{\rm CB}}{R} & \text{outside } R_{\rm CB} \end{cases} \tag{4}$$

Here, the normalization value ${\rm RM}_o \equiv n_{{\rm e}o} B_{zo} h_o$ is taken to be equal to 1×10^5 rad/m^2. For simplicity, these approximate expressions ignore the internal Faraday depolarization although several models considered in EHT VIII [2] (see [6]) indicate that Faraday depo-

larization in the midplane is strong. We also ignore any contribution to the line-of-sight magnetic field and to the RM from the turbulent magnetic field in the disk. However, we note that the GRMHD numerical simulations of [6] showed that there are periods during the evolution of the system that the turbulent magnetic field may dominate the RM, thus our expressions may be valid only on average, and during a period of quiescent (non-turbulent) disk activity.

The M87* disk is not observed face-on, thus photons emitted from the disk that reach the EHT observer cross the disk at some nonzero angle χ from the vertical to the disk (see Figure 1). For simplicity, we will only consider the line-of-sight contribution of the axial field B_z in the RM map, and ignore the line-of-sight contribution of the field in the equatorial plane of the disk. As we just acknowledged, this is not always true. Under this simplifying approximation, the local contribution to the RM from a path length ds through the thin disk is equal to $n_{\rm e} B_{\rm line-of-sight} {\rm d}s = n_{\rm e} B_z \cos\chi \, (h/\cos\chi) = n_{\rm e} B_z h$, thus

$$\mathrm{RM}(R,\phi) \quad \approx \quad \mathrm{RM}_{\rm face-on}(R) \tag{5}$$

In order to obtain RM maps on the sky, we will follow the approximate analytical formulation provided by Beloborodov [13] and most recently by Narayan et al. [14] to account for the geodesics of photons emitted from the M87* disk that reach the EHT observer on earth. According to Narayan et al. [14], each point (R,ϕ) in the disk is mapped onto

$$\begin{aligned} x(R,\phi) &= (R+1)\cos\phi \\ &\quad -\frac{1}{2R}\cos\phi + \sin\theta_o \sin^2\phi - \frac{R}{2}\sin^2\theta_o \sin^2\phi\cos\phi \end{aligned} \tag{6}$$

$$\begin{aligned} y(R,\phi) &= (R+1)\sin\phi \\ &\quad -\frac{1}{2R}\sin\phi + 2\sin\theta_o \sin^2\phi - \frac{R}{2}\sin^2\theta_o \sin^3\phi \end{aligned} \tag{7}$$

on the plane of the sky, where R, x, y are expressed in units of GM/c^2 (M is the mass of the black hole, G is Newton's constant, and c is the speed of light). x is measured along the line of nodes of the plane of the disk along $\phi = 0$, and y is measured perpendicularly to it along $\phi = 90^\circ$. $\theta_o = 17^\circ$ is the inclination of the M87* disk with respect to our line of sight. Note that the line of nodes is tilted with respect to the East-West horizontal on the sky by 72° clockwise. We have tacitly assumed here that the direction of the large scale jet in the galaxy M87 coincides with the z-direction perpendicular to the accretion disk around the central black hole in M87*. Obviously, the two may differ.

As we acknowledged above, the distance $R_{\rm CB}$ is currently a big unknown. If we choose the distance of field reversal to concide with the position of the light emitting ring in the EHT image, namely $R_{\rm CB} = 4.5 GM/c^2$ [14], we obtain the theoretical RM map shown in Figure 2.

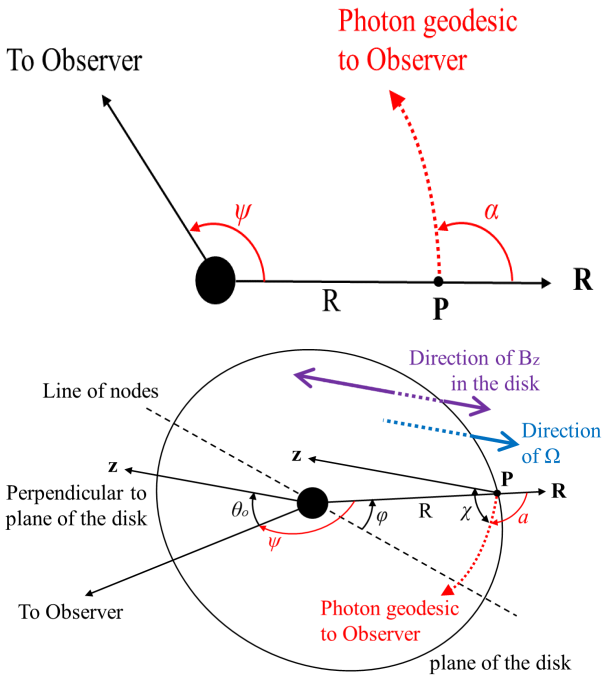

Figure 1. Top: angles ψ and α along the geodesic plane that is defined by the lines connecting the central black hole to the photon emitting point P at distance R, and to the EHT observer (same notation as in [14]); Bottom: 3D view of the geodesic plane in relation to the plane of the disk. $\theta_o = 17°$. ϕ is defined counter-clockwise from the line of nodes of the plane of the disk. Both Ω and B_z lie along **z**. Notice that the z-direction perpendicular to the disk is drawn twice: at the position of the central black hole, and at the position of the photon emitting point P. The photon trajectory makes an angle χ with the vertical z-direction at its point of origin in the disk. As defined in this sketch, $\Omega < 0$ for the particular viewing angle of M87*, and according to the Cosmic Battery prescription, $B_z < 0$ inside $R_{\rm CB}$, and $B_z > 0$ outside (as we noted in the text, the position of field reversal is not known; here, we have assumed for simplicity that it is at $R_{\rm CB} = R_{\rm CB}$). The geodesic plane makes an angle ξ (not shown) with respect to the disk plane around the line connecting the central black hole to the photon emitting point P.

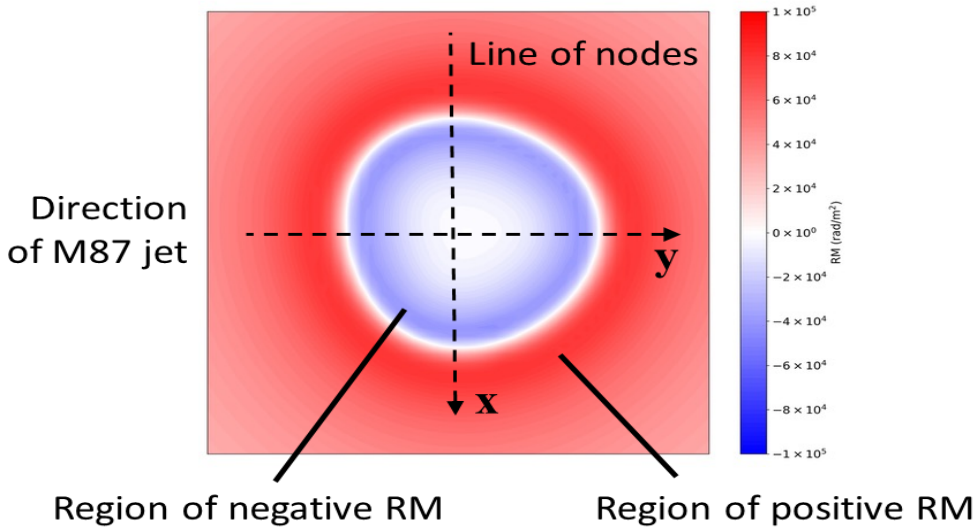

Figure 2. RM map according to the Cosmic Battery described through Equations (5)–(7). The distance of field reversal is assumed at $R_{\rm CB} = 4.5GM/c^2$.

3. Rapid RM Reversals

In order to generate RM maps, we need simultaneous knowledge of the Electric Vector Polarization Angles (EVPAs) in the high and low bands of the EHT polarization maps. The RM value at each point of the polarization map is determined as

$$\begin{aligned} \mathrm{RM} &= \frac{\mathrm{EVPA_{low}} - \mathrm{EVPA_{high}}}{\lambda^2_{\mathrm{low}} - \lambda^2_{\mathrm{high}}} \\ &= 5.8 \times 10^5 \left(\mathrm{EVPA_{low}} - \mathrm{EVPA_{high}}\right) \mathrm{rad/m^2}\,. \end{aligned} \tag{8}$$

Here, EVPAs are measured in degrees counter-clockwise from North (up), and "low"/"high" refer to the so-called low/high band observations of EHT at 227.1/229.1 GHz respectively. Although the raw EVPA data is not yet available from the EHT collaboration, a direct visual inspection of the fiducial M87* daily average maps shown in Figure 28 of EHT VII [1] reveals EVPA differences between the low and high bands of up to about 10°, corresponding to RM values on the order of 10^6 rad/m^2, i.e., much higher than the expected contribution of foreground Faraday screens and the contribution of our own Galaxy which are all expected to be on the order of only 10^2 rad/m^2. Therefore, at the resolution of EHT the sign (positive/negative) of the RM values calculated directly through Equation (8) represent the direction of the line-of-sight magnetic field (towards us/away from us respectively). The above visual inspection revealed various regions around M87* with either positive or negative differences between the EVPA of the two bands ($\mathrm{EVPA_{low}} - \mathrm{EVPA_{high}}$), corresponding to positive and negative RM values, respectively, as described in Equation (8). However, the uncertainty of the EVPA measurements is probably of the order of $\pm 10°$ (e.g., see Figure 8 of EHT VII [1]), which is similar to the EVPA differences betwen the low and high bands, and hence the RM sign cannot be reliably constrained by the visual inspection of the EHT polarization images of M87* described above. Nevertheless, we plan to perform detailed RM investigations as soon as the raw EVPA data become available.

One way to improve this unfortunate situation is to look at the average RM values. The published average RM values for the four days 5, 6, 10, and 11 April 2017 of EHT observations, as constrained with ALMA observations at 1.3 mm and 3 mm are 0.64 ± 0.27, 1.51 ± 0.29, -0.32 ± 0.24, $-0.41 \pm 0.23 \times 10^5$ rad/m^2 respectively Goddi et al. [5]. Since we are primarily interested in the sign of the line-of-sight magnetic fields, i.e., the sign in the RM maps, the above average RM values suggest that the RM sign of the polarization image alternates within a few days. This is a suggestion that the accretion disk in the immediate vicinity of the central black hole is threaded by both positive and negative vertical magnetic field B_z over extended parts of the inner disk. Similar transient structures have also been observed in the canonical MAD GRMHD simulations performed by the EHT Collaboration to account for the overall features of the EHT image of M87* [6]. The initial conditions in these simulations assume a large scale axial magnetic field in the accretion disk that is unidirectional, i.e., *without* field reversals. Other researchers favor initial configurations *with* field reversals (e.g., [15]). Nevertheless, the fact that the turbulence in the disk can induce transient axial field reversals even in numerical simulations without initial field reversals, leads us to accept that the observation of RM sign flips in the EHT polarization images does not yet consist confirmation of the Cosmic Battery.

4. Conclusions

Confirmation of the Cosmic Battery would consist of observing a large-scale pattern of alternating field polarities similar to the one shown in Figure 2 over several EHT observing periods with no transient RM sign flips. One possibility is that the interface between the two B_z polarities does not have the well-defined compact shape shown in Figure 2, with "tongues" of alternating sign RM contributing to the observed RM values. In other words, it is not only the instantaneous RM map morphology that matters, but also its day-to-day variability. The determination of a large scale geometry such as that of Figure 2 may require

either a longer term monitoring, in order to determine an average value of the RM as a function of distance from the black hole, or even the synergy with lower resolution RM observations that can capture the spatial average of such a topology at both small and large scales.

The published EHT observations in the low and high bands cover a very narrow region of the RM space and hence they are insensitive to lower RM values which can be manifested by observations over a wider range of frequencies. This is more relevant for regions of low density plasma and/or low magnetic field strengths which give rise to the lower RM values. Such regions may belong to larger spatial scales where the field pattern predicted by the Cosmic Battery may be easier to detect. If indeed we observe an average pattern similar to the one shown in Figure 2, this would be a hint that the standard scenario according to which the magnetic field that threads the disk is brought in from large distances and saturates in the immediate vicinity of the central black hole with one and the same polarity *may not work*. The alternative is that dipolar magnetic flux of both polarities is generated locally by some physical mechanism like the one we propose in this paper. While it appears currently difficult to establish the average large-scale geometry of the near black hole axial field, we believe these observations present an interesting first step in this direction, with the hope future refinements will allow us to reach this goal.

It is interesting that the reversal of the magnetic field polarity at some distance from the central black hole will correspond to a *large scale current sheet*. This configuration is expected to lead to several important features such as dynamic intermittent behavior with continuous reconnection and plasmoid formation along it. This may be a fundamental element of astrophysical jets according to several theoretical models of magnetically driven jets and winds (e.g., [16]). The current sheet may naturally account for several characteristic features of AGN jets such as particle acceleration and enhanced radiation emission along its direction (as is the case with the pulsar curent sheet [17]), 180° polarization angle swings as it sweeps the observer's line-of-sight (e.g., [18]), etc. Another important feature is that since there is a limited amount of magnetic flux threading the innermost accretion disk around the central black hole, the magnetic flux of the opposite (return) polarity threading the large scale disk is also limited. Therefore, for the return flux to fill the whole accretion disk, the magnetic field immediately outside the distance of field reversal will drop. We thus predict a region of weaker magnetic field (and thus also weaker synchrotron emission) surrounding the jet [19]. This may be one of the reasons AGN jets have this characteristic sheath structure.

Time and more observations will tell if we will ever be able to observe the Cosmic Battery magnetic field configuration and the footpoint of the purported current sheet along the surface of the core jet in M87*.

Author Contributions: Writing—original draft preparation, I.C.; writing—review and editing, I.M., D.K. and A.N. All authors have read and agreed to the published version of the manuscript.

Funding: This research received no external funding.

Conflicts of Interest: The authors declare no conflict of interest.

Note

[1] During the preparation of this work, the first image of the shadow of Sgr A* (the supermassive black hole in the center of the Milky Way) was obtained by the EHT Collaboration [4]. Preliminary model fitting of the EHT image favors an accretion disk viewed at low inclination ($i < 50°$). This makes Sgr A* one more interesting target for testing the Cosmic Battery model, provided the direction of Ω of the disk is also determined.

References

1. The Event Horizon Telescope Colaboration. First M87 Event Horizon Telescope Results. VII. Polarization of the Ring. *Astrophys. J. Lett.* **2021**, *910*, L12. [CrossRef]
2. The Event Horizon Telescope Colaboration. First M87 Event Horizon Telescope Results. VIII. Magnetic Field Structure near the Event Horizon. *Astrophys. J. Lett.* **2021**, *910*, L13. [CrossRef]

3. Walker, R.C.; Hardee, P.E.; Davies, F.B.; Ly, C.; Junor, W. The Structure and Dynamics of the Subparsec Jet in M87 Based on 50 VLBA Observations over 17 Years at 43 GHz. *Astrophys. J.* **2018**, *855*, 128. [CrossRef]
4. The Event Horizon Telescope Colaboration. First Sagittarius A* Event Horizon Telescope Results. I. The Shadow of the Supermassive Black Hole in the Center of the Milky Way. *Astrophys. J. Lett.* **2022**, *930*, L12. [CrossRef]
5. Goddi, C.; Zhao, G.; Gómez, J.L.; Fuentes, A.; Krichbaum, T.P.; Traianou, E.; Lico, R.; Cho, I.; Ros, E.; Komossa, S.; et al. Unraveling the Innermost Jet Structure of OJ 287 with the First GMVA + ALMA Observations. *Astrophys. J.* **2021**, *910L*, 14. [CrossRef]
6. Ricarte, A.; Prather, B.S.; Wong, G.N.; Narayan, R.; Gammie, C.; Johnson, M. Decomposing the Internal Faraday Rotation of Black Hole Accretion Flows. *Mon. Not. R. Astron. Soc.* **2020**, *498*, 5468. [CrossRef]
7. Contopoulos, I.; Kazanas, D. A Cosmic Battery. *Astrophys. J.* **1998**, *508*, 859. [CrossRef]
8. Lynden-Bell, D. Magnetism Along Spin. *Observatory* **2013**, *133*, 266–269.
9. Christodoulou, D.M.; Gabuzda, D.C.; Knuettel, S.; Contopoulos, I.; Kazanas, D.; Coughlan, C.P. Dominance of outflowing electric currents on decaparsec to kiloparsec scales in extragalactic jets. *Astron. Astrophys.* **2016**, *591*, A61. [CrossRef]
10. Myserlis, I. An underlying universal pattern in galaxy halo magnetic fields Contopoulos, I. *Astron. Astrophys.* **2021**, *649*, 94. [CrossRef]
11. Contopoulos, I.; Kazanas, D.; Fukumura, K. Magnetically Advected Winds *Nat. Astron.* **2017**, *1*, 62.
12. Contopoulos, I.; Nathanail, A.; Sadowski, A.; Kazanas, D.; Narayan, R. Numerical simulations of the Cosmic Battery in accretion flows around astrophysical black holes. *Mon. Not. R. Astron. Soc.* **2018**, *473*, 721. [CrossRef]
13. Beloborodov, A.M. Gravitational Bending of Light Near Compact Objects. *Astrophys. J.* **2002**, *566*, L85. [CrossRef]
14. Narayan, R.; Palumbo, D.C.M.; Johnson, M.D.; Gelles, Z.; Himwich, E.; Chang, D.O.; Ricarte, A.; Dexter, J.; Gammie, C.F.; Chael, A.A. The Polarized Image of a Synchrotron-emitting Ring of Gas Orbiting a Black Hole. *Astrophys. J.* **2021**, *912*, 35. [CrossRef]
15. Nathanail, A.; Fromm, C.M.; Porth, O.; Olivares, H.; Younsi, Z.; Mizuno, Y.; Rezzolla, L. Modelling the polarised emission from black holes on event horizon-scales. *Mon. Not. R. Astron. Soc.* **2020**, *495*, 3780. [CrossRef]
16. Nathanail, A.; Contopoulos, I. Black Hole Magnetospheres. *Astrophys. J.* **2014**, *788*, 186. [CrossRef]
17. Kalapotharakos, C.; Brambilla, G.; Timokhin, A.; Harding, A.K.; Kazanas, D. Three-dimensional Kinetic Pulsar Magnetosphere Models: Connecting to Gamma-Ray Observations. *Astrophys. J.* **2018**, *857*, 44. [CrossRef]
18. Blinov, D.; Kiehlmann, S.; Pavlidou, V.; Panopoulou, G.V.; Skalidis, R.; Angelakis, E.; Casadio, C.; Einoder, E.N.; Hovatta, T.; Kokolakis, A.K.; et al. RoboPol: AGN polarimetric monitoring data. *Mon. Not. R. Astron. Soc.* **2021**, *501*, 3715. [CrossRef]
19. Contopoulos, I. The immediate environment of an astrophysical black hole. *Mon. Not. R. Astron. Soc.* **2018**, *473*, L146. [CrossRef]